

# Northumbria Research Link

Citation: Zhang, Qian, Wang, Yong, Wang, Tao, Li, Dongsheng, Xie, Jin, Torun, Hamdi and Fu, Yong Qing (2021) Flexible Smart Acoustic Wave Patches for Effective Detection and Elimination of Surface Condensation. In: 2021 21st International Conference on Solid-State Sensors, Actuators and Microsystems (Transducers). IEEE, Piscataway, pp. 1263-1266. ISBN 9781665448451, 9781665412674

Published by: IEEE

URL: <https://doi.org/10.1109/Transducers50396.2021.9495501>  
<<https://doi.org/10.1109/Transducers50396.2021.9495501>>

This version was downloaded from Northumbria Research Link:  
<http://nrl.northumbria.ac.uk/id/eprint/47528/>

Northumbria University has developed Northumbria Research Link (NRL) to enable users to access the University's research output. Copyright © and moral rights for items on NRL are retained by the individual author(s) and/or other copyright owners. Single copies of full items can be reproduced, displayed or performed, and given to third parties in any format or medium for personal research or study, educational, or not-for-profit purposes without prior permission or charge, provided the authors, title and full bibliographic details are given, as well as a hyperlink and/or URL to the original metadata page. The content must not be changed in any way. Full items must not be sold commercially in any format or medium without formal permission of the copyright holder. The full policy is available online: <http://nrl.northumbria.ac.uk/policies.html>

This document may differ from the final, published version of the research and has been made available online in accordance with publisher policies. To read and/or cite from the published version of the research, please visit the publisher's website (a subscription may be required.)

# FLEXIBLE SMART ACOUSTIC WAVE PATCHES FOR EFFECTIVE DETECTION AND ELIMINATION OF SURFACE CONDENSATION

Qian Zhang<sup>1,2</sup>, Yong Wang<sup>1,2,3</sup>, Tao Wang<sup>1</sup>, Dongsheng Li<sup>1</sup>, Jin Xie<sup>1,\*</sup>, Hamdi Torun,<sup>2</sup> and YongQing Fu<sup>2,\*</sup>

<sup>1</sup>State Key Laboratory of Fluid Power and Mechatronic Systems, Zhejiang University, Hangzhou 310027, China

<sup>2</sup>Faculty of Engineering and Environment, University of Northumbria, Newcastle upon Tyne NE1 8ST, UK and

<sup>3</sup>Key Laboratory of 3D Micro/Nano Fabrication and Characterization of Zhejiang Province, School of Engineering, Westlake University, Hangzhou 310024, China

## ABSTRACT

In this paper, flexible ZnO/Al Lamb wave device was used to detect and eliminate surface condensations, commonly occurring in chemical process, agriculture, automobile and pipelines. The flexible and smart patch based on acoustic wave devices can identify dew formation through the change of frequency spectrum and then actuate to remove the condensation through acousto-thermal effect. To distinguish the differences between environmental interference (temperature and humidity) and the real condensation, a specified 3D space was built to quantify the degree of distortion of the transmission spectra. For droplets uniformly distributed on the surface of the device with an input power of  $\sim 0.6$  W, the evaporation time was significantly reduced to  $\sim 1/13$  of the natural evaporation time.

## KEYWORDS

Flexible smart patches, Condensation detection and elimination, Lamb wave

## INTRODUCTION

Condensation is a ubiquitous phenomenon in industrial production, scientific research and daily life [1, 2]. It can be utilized in the sensing of respiration [3], humidity [4] and dew point [5], where small droplets are condensed on the surface, which changes the mass loading and electrical characteristics. Nevertheless, it sometimes can become problematic and even harmful in applications such as agriculture [5], automobile [6] and coal-fired power plants [7]. Various detection methodologies have been developed in recent years, including surface plasmon resonance (SPR) [8], surface acoustic wave (SAW) [9], micro galvanic-coupled arrays [10] and quartz crystal resonator (QCR) [5]. However, attention has not been paid for the fast detection and elimination of condensation using an effective method.

In this paper, we report a flexible and smart patch which can detect and then eliminate condensation using acoustic wave technique based on piezoelectric ZnO thin film coated onto flexible aluminum (Al) substrate. The working principle can be explained as follows. The small droplets formed onto the device due to the condensation lead to the energy dissipation of acoustic waves, which can be monitored from the amplitude changes of their transmission spectra (S21). Excited by an alternating current (AC), the acoustic wave device can generate local heating due to the acousto-thermal effect [11]. Owing to

the excellent thermal conductivity of the Al substrate, the surface temperature of the whole device will rise, which effectively eliminate or prevent the condensation.

In this study, we will explore using the ZnO/Al flexible acoustic wave device to detect and eliminate the dew condensation. Temperature and humidity are two main interferences for the condensation detection. We have conducted experiments where only temperature or humidity is changed, and the results are compared with those of condensation experiments which can distinguish the variations of transmission spectra caused by the condensation and its interferences (e.g., temperature and humidity). For elimination of the condensation, the SAW device takes  $\sim 1/13$  of the time for the small droplets to evaporate completely compared to natural evaporation if an acoustic wave power of  $\sim 0.6$  W (24.9 MHz) is applied. In addition, if there is no dew formation, we show that the condensation can be effectively prevented using the same amount of input power.

## EXPERIMENTAL SETUP

The flexible device was fabricated by depositing ZnO thin film ( $\sim 5$   $\mu\text{m}$  thick) onto commercially available Al foil (50  $\mu\text{m}$  thick). With a wavelength of 100  $\mu\text{m}$ , the Al interdigital transducers (IDTs) were fabricated onto ZnO using a standard lithography and lift-off process. The device can excite Lamb waves including A0, S0, A1, S1 modes. The A0 mode was adopted in the experiments owing to its relatively low noise.

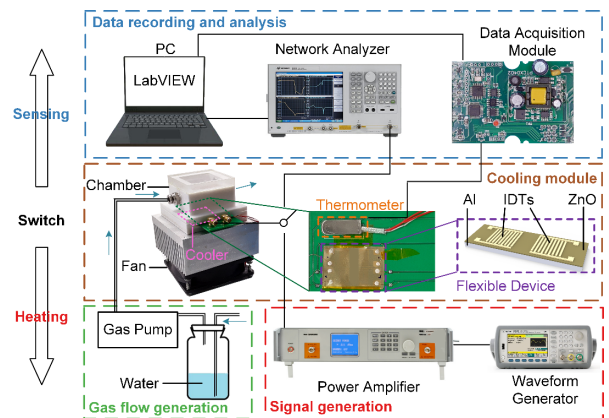


Figure 1: Experimental setup used for the temperature, humidity and condensation control tests. The flexible device can be switched to sensing mode by connecting to a network analyzer, and to heating mode by connecting to a power amplifier and a waveform generator.

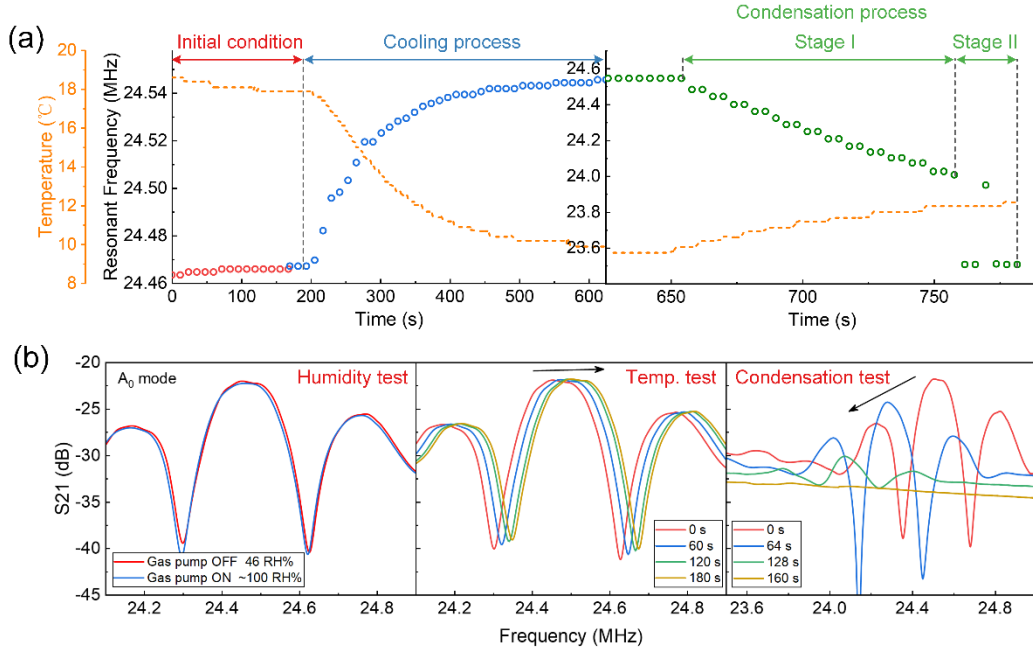


Figure 2: (a) Real-time resonant frequencies of A0 mode and temperatures recorded in the temperature and condensation control tests. The transmission spectra of A0 mode in the (b) humidity, (c) temperature and (d) condensation control tests.

As shown in Fig. 1, the flexible ZnO/Al device and a thermometer (PT 100) were taped on a printed circuit board (PCB), which was placed in a closed chamber. To generate condensation, a thermoelectric cooler at the bottom of the chamber was used to control the substrate temperature, and a pump with a gas-washing bottle was used to generate moist airflow (~100 RH%). By connecting the flexible ZnO/Al device to a network analyzer (sensing mode) or a power amplifier (heating mode), both the functions of detection and elimination of condensation can be realized. In the sensing mode, the vector network analyzer (Agilent E5061B) and a data acquisition module were used to measure the S parameters of the ZnO/Al device and the resistance of the thermometer respectively, which were then synchronously recorded using a LabVIEW program. In the heating mode, sinusoidal signals with a frequency of 24.9 MHz were generated by a waveform generator (Agilent 33522A), amplified by a power amplifier (MWPA100K) and then fed into the IDTs.

In order to distinguish condensation and other interferences (i.e., temperature and humidity), three groups of experiments were conducted, including temperature control test, humidity control test and condensation control test. In the humidity control test, the pump was turned on and the cooler was turned off so that only humidity has been changed while the other parameters were remained the similar values. On the contrary, in the temperature control test, the gas pump was turned off and the cooler was turned on so that only the temperature was changed. The condensation control test was carried out keeping both the gas pump and cooler on to generate dew condensation.

## RESULTS AND DISCUSSION

### Detection of condensation

Fig. 2(a) shows the resonant frequencies (A0 mode) and temperature variations in the cooling and condensation

tests. In the cooling (temperature) tests, with the decrease of temperature (up to 8 °C), the resonant frequency increases gradually (up to 79 kHz) until reaching a plateau. In the subsequent condensation test, the temperature increases slightly (~2.6 °C) because the airflow accelerates the heat exchange, thus resulting in a slightly higher equilibrium temperature. At the same time, the resonant frequency decreases (540 kHz) due to the condensation on the surface in the early stage (stage I). With the increase of condensed droplets accumulated on the surface, the amplitude of resonance peak gradually decreases and eventually disappear. At this stage, the monitoring of resonant frequency is meaningless (stage II). Figs. 2(b) to 2(d) show the transmission spectra of A0 mode in the humidity control, temperature control and condensation control tests, respectively. The humidity change (46 RH% to ~100 RH%) does not induce significant changes of the transmission spectra. The decrease of temperature (~6 °C) results in changes of the resonant frequency, while the condensation process causes significant changes of both the resonant frequency and amplitude of the transmission spectra.

However, it's difficult to determine whether the generation of condensation simply using shifts of resonant frequency. To further distinguish the condensation and their interferences, the transmission spectra (amplitude-frequency) in a frequency range (23.5 MHz to 25.5 MHz), which consists of 1601 points, are taken for the analysis. However, the 1601 amplitudes compose a 1601-dimensional vector which is inconvenient for data processing. Three amplitude-related features are selected to reduce the dimension of the high-dimensional vectors, including maximum amplitude, peak-to-peak amplitude and "distance". Here the "distance" is defined as the Euclidean distance between a certain vector and reference vector after the alignment of their resonant peaks, indicating the accumulated distortion of transmission

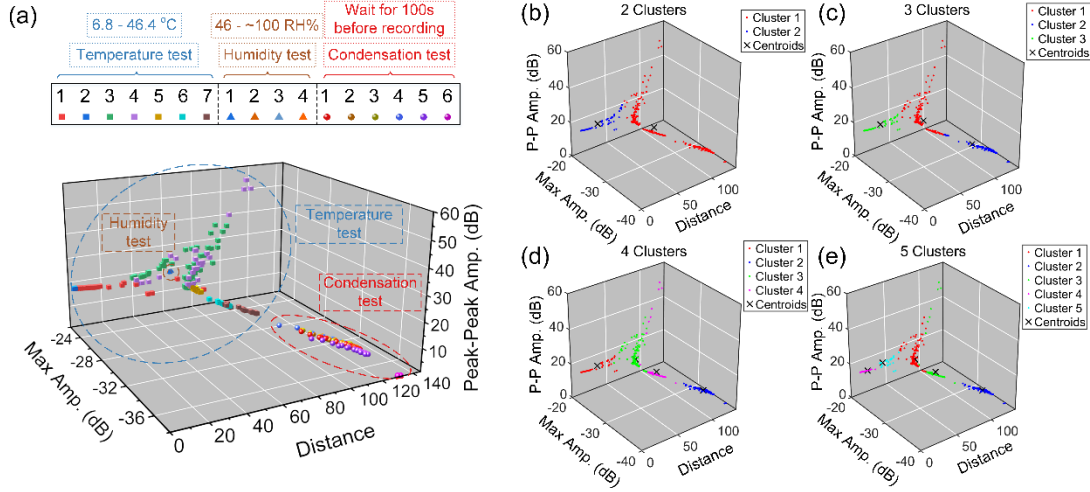


Figure 3: (a) After dimensionality reduction, the transfer spectra of  $A_0$  mode recorded in the temperature, humidity and condensation control tests are mapped to the specifically defined 3-dimensional space. Classification for the points in (a) using K-means algorithm with (b) 2 clusters, (c) 3 clusters, (d) 4 clusters and (e) 5 clusters.

spectrum. The reference vector is recorded at room temperature ( $\sim 14$  °C) and humidity (46 RH%) which is regarded as the origin of the 1601-dimensional space.

As shown in Fig. 3(a), the three axes are the maximum amplitude, the peak-to-peak amplitude and the “distance”, respectively. Every point in this 3D space corresponds to a 1601-dimensional vector recorded in the temperature control, humidity control, or condensation control test. Intuitively, we can distinguish the condensation process from other disturbances (temperature and humidity). To further investigate the effectiveness of the 3 features, K-means clustering algorithm [12] was adopted with cluster numbers of 2, 3, 4 and 5, and the results are shown in Figs. 3(b) to 3(e). With a cluster number larger than 3, the data points obtained in the condensation tests can be divided into a separate cluster (blue), indicating their significant differences in spatial coordinates. The centroid is defined as the weighted average of the coordinates of all points in a cluster. Here the weight of each point is equal. In the actual measurement, we only need to read the  $S_{21}$  spectrum, reduce its dimension to obtain the values of three features which are regarded as the coordinates of a new point, and finally calculate the Euclidean distance between the new point and the several (e.g., 4) known centroids. The closer to a centroid, the more likely the new point belongs to the corresponding cluster. As a result, we can accurately determine whether condensation occurs.

### Elimination and prevention of condensation

The heating mode is investigated for the elimination and prevention of condensation. Figs. 4(a) and 4(b) show the photos of the evaporation process of condensations with and without input of power ( $\sim 0.6$  W, 24.9 MHz). The room temperature and humidity are  $\sim 18$  °C and  $\sim 46$  RH%, respectively. It takes  $\sim 50$  s for the condensations generated in the condensation control tests fully removed under the heating mode, which is only  $\sim 1/13$  of that in the natural condition ( $\sim 640$  s). As shown in Fig. 4(c), the experiments were conducted with both the pump and cooler on for  $\sim 200$  s. The heating mode can effectively prevent the condensation, which can be verified from the image of the dry surface of the sample and the  $S_{21}$  spectrum (red curve).

On the other hand, without the power input, there are dense small droplets on the surface, and the intensity of  $S_{21}$  spectrum reduces (green curve).

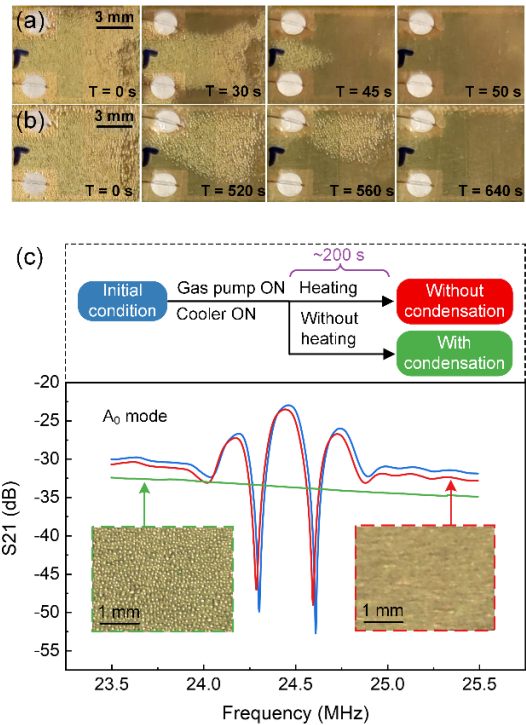


Figure 4: Photos of the evaporation process of the condensation on the surface of the flexible ZnO/Al device (a) with power input ( $\sim 0.6$  W) and (b) without power input. (c) After turning on the gas pump and cooler for  $\sim 200$  s, the  $S_{21}$  spectra and photos of the ZnO/Al device with and without power input ( $\sim 0.6$  W).

### CONCLUSION

In summary, we present a flexible ZnO/Al acoustic wave device for detecting and eliminating the dew condensation on its surface. We also proposed a new methodology of building a specified 3D space to identify

the condensation by analyzing the degree of distortion of the transmission spectra. With an input power of  $\sim 0.6$  W, the evaporation time of droplets is dramatically reduced from  $\sim 640$  s to  $\sim 50$  s owing to the acousto-thermal effect. Furthermore, the condensation can be effectively prevented with the same input power. The flexible smart patch is promising in various applications where curved surfaces are involved, e.g., leaves and branches of plants to monitor their growth environment, pipeline walls which are prone to corrosion by condensation, windshields of automobiles where condensation may obscure driver's vision.

### ACKNOWLEDGEMENTS

This work was financially supported by the "National Natural Science Foundation of China (51875521)", the "Zhejiang Provincial Natural Science Foundation of China (LZ19E050002)", the "Science Fund for Creative Research Groups of National Natural Science Foundation of China (51821093)", the UK Engineering, and Physical Sciences Research Council (EPSRC) grants EP/P018998/1, and Special Interests Group of Acoustofluidics under the EPSRC-funded UK Fluidic Network (EP/N032861/1).

### REFERENCES

[1] H. Cha et al., "Dropwise condensation on solid hydrophilic surfaces," *Sci. Adv.*, vol. 6, no. 2, eaax0746, 2020.

[2] Q. Yang et al., "Capillary condensation under atomic-scale confinement," *Nature*, vol. 588, no. 7837, pp. 250–253, 2020.

[3] Y. Guan et al., "A universal respiration sensing platform utilizing surface water condensation," *J. Mater. Chem. C*, vol. 7, no. 10, pp. 2853–2864, 2019.

[4] Y. Q. Wei, B. J. Bailey, and B.C. Stenning, "A wetness sensor for detecting condensation on tomato plants in green house," *J. agric. Engng Res.*, vol. 61, pp. 197–204, 1995.

[5] J. Nie, J. Liu, N. Li, and X. Meng, "Dew point measurement using dual quartz crystal resonator sensor," *Sensors Actuators, B Chem.*, vol. 246, pp. 792–799, 2017.

[6] D. Gould, M. Meiners, W. Benecke, and W. Lang, "Condensation detection using a wirelessly powered RF-temperature sensor," *IEEE Trans. Veh. Technol.*, vol. 58, no. 4, pp. 1667–1672, 2009.

[7] Y. Li et al., "Method of flash evaporation and condensation - heat pump for deep cooling of coal-fired power plant flue gas: Latent heat and water recovery," *Appl. Energy*, vol. 172, pp. 107–117, 2016.

[8] K. Iwami et al., "Plasmon-resonance dew condensation sensor made of gold-ceramic nanocomposite and its application in condensation prevention," *Sensors Actuators, B Chem.*, vol. 184, pp. 301–305, 2013.

[9] K. A. Vetelino, P. R. Story, R. D. Mileham, and D. W. Galipeau, "Improved dew point measurements based on a SAW sensor," *Sensors Actuators, B Chem.*, vol. 35, no. 1–3, pp. 91–98, 1996.

[10] Y. Kubota, V. L. Mishra, T. Ando, Y. Sakamoto, and J. Kawakita, "Micro/nano galvanic-coupled arrays for early and initial detection and prediction of dew condensation," *Sensors Actuators, A Phys.*, vol. 303, p. 111838, 2020.

[11] Y. Wang et al., "A rapid and controllable acoustothermal microheater using thin film surface acoustic waves," *Sensors Actuators, A Phys.*, vol. 318, p. 112508, 2021.

[12] K. A. Abdul Nazeer and M. P. Sebastian, "Improving the Accuracy and Efficiency of the k-means Clustering Algorithm," *Proc. World Congr. Eng. London, WCE*, vol. 1, no. May, pp. 1–5, 2001.

### CONTACT

\* xiejin@zju.edu.cn; richard.fu@northumbria.ac.uk